

COSMIC SHEAR WITH THE VLT

R. MAOLI^{1,2}, Y. MELLIER², L. VAN WAERBEKE^{2,3}, P. SCHNEIDER^{4,5},
B. JAIN⁶, T. ERBEN⁵, F. BERNARDEAU⁷, B. FORT²

¹ *Dipartimento di Fisica, Università di "Roma La Sapienza", Italy*

² *Institut d'Astrophysique de Paris, France*

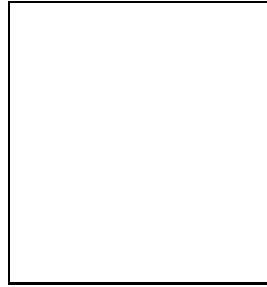
³ *Canadian Institute for Theoretical Astrophysics, Toronto, Canada*

⁴ *Institut für Astrophysik und Extraterrestrische Forschung, Bonn, Germany*

⁵ *Max Planck Institut für Astrophysik, Garching, Germany*

⁶ *Department of Physics, Johns Hopkins University, Baltimore, USA*

⁷ *Service de Physique Théorique, C.E. de Saclay, France*



We report on the detection of cosmic shear on angular scales of 1.3-6.5 arcmin using 45 independent empty fields observed with the Very Large Telescope (VLT). This result confirms previous measurements obtained with the CFH Telescope at the same angular scales. We present the data analysis and the first preliminary results.

1 Introduction

The large scale structures of the Universe induce gravitational distortion of the shape of the background galaxies which can be observed on CCD images as a correlated ellipticity distribution of the lensed sources (the cosmic shear). The analysis of cosmic shear permits to extract information on the geometry of space (Ω and λ) as well as on the power spectrum of the (dark) matter density perturbations responsible for the distortion. Therefore, it directly compares observations with cosmological models, without regards on the light distribution.

In contrast to weak lensing analysis of clusters of galaxies, measuring cosmic shear is still a challenge. It has a very small amplitude (≈ 5 times lower than in clusters) and demands deep images of a large portion of the sky obtained with high precision instruments. Up to now, this task was beyond the reach of the available technology. Although a first detection in a blank sky region was reported two years ago¹, it is only recently that four different groups have succeeded in observing cosmic shear^{2, 3, 4, 5}.

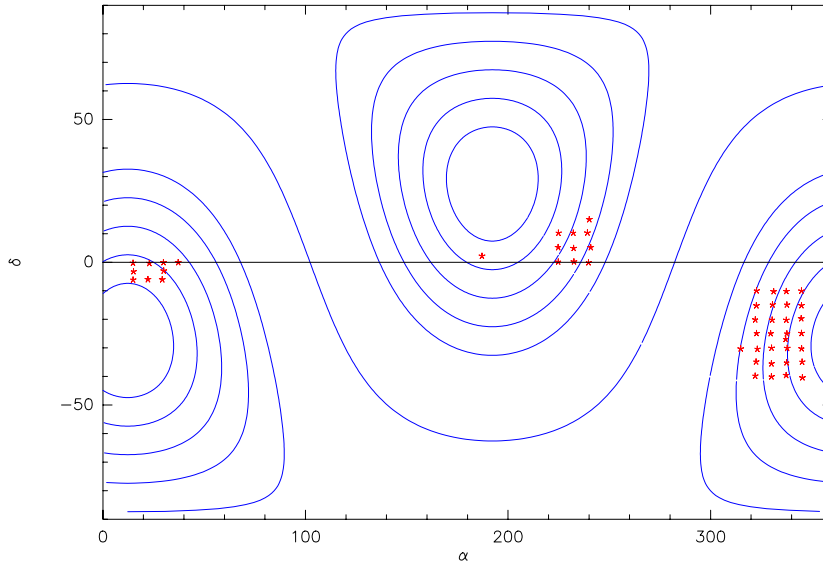


Figure 1: Distribution on the sky of the 50 VLT fields. Continuous lines are for galactic latitudes $b = 0, \pm 30, \pm 40, \pm 50, \pm 60, \pm 70$. Contrary to what it can seem to a first look, they are not on a regular grid.

The critical issues regarding the reliability of the cosmic shear measurement are the three sources of noise:

- intrinsic noise
- systematics
- cosmic variance

Minimizing the first one is important to get a significant detection; understanding and controlling the second one is important to be sure that the signal is induced by cosmic shear; then minimizing the third one is important to compare the signal with cosmological scenarios.

By using jointly these detections it is possible to rule out some scenarios. However, the cosmic variance is still too large to distinguish among the more common models of the Universe. A significant improvement implies the observation of many independent fields. The Cambridge group³ used nearly statistical independent areas of the sky, but has only 13 fields. The other experiments cover a larger area but sample compact regions with few independent fields. In this case the amplitude of the cosmic variance is estimated by running numerical simulations for each current cosmological models. In any case, the cosmic variance is greater than in the case of observation of completely statistical independent fields. The alternative is to observe many independent fields in order to infer the cosmic variance from the fluctuations of the shear observed from field-to-field. This is the strategy we developed with the VLT/FORS1 survey. In the following, we describe the analysis of cosmic shear in 50 FORS1 fields. This is a preliminary study which does not include an extensive investigation of systematics. Nevertheless, the signal is strong and highly significant, so we are confident in the results shown in this proceeding.

2 Observational strategy analysis of VLT/FORS1 data

All the data were obtained in the I band with the FORS1 instrument, a 2048×2048 pixel CCD with a $6.8'$ field of view, mounted at the Cassegrain focus of the VLT-UT1.

- In figure 1 we plot the sky distribution of the 50 VLT fields. Their main characteristics are:
- at least 5 degrees of separation, to be statistically independent;
 - absence of bright stars ($m_B > 14$), to avoid diffraction spikes and light scattering;

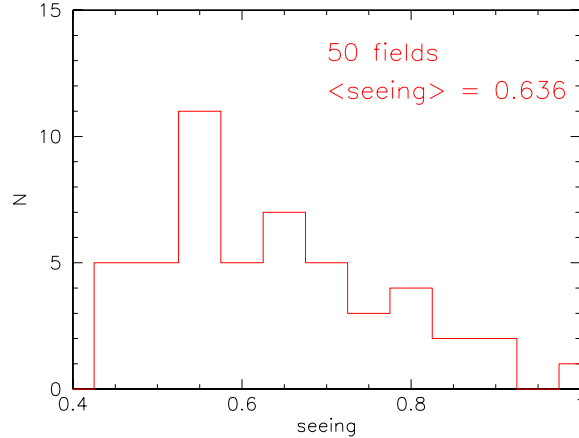


Figure 2: Histogram of the seeing for the 50 final coadded fields.

- intermediate galactic latitudes ($30^\circ \leq b \leq 70^\circ$), to have enough stars for the PSF correction;
- two fields in common with the HST/STIS project and two with the WHT project, to allow for cross checking of the results.

Observations were made between May and September 1999 using the service mode available at ESO. This observing strategy is particularly well suited for cosmic shear surveys, ensuring a seeing always lower than $0.8''$ and taking advantage from the possibility to spread the targets over a very large part of the sky.

Each field was observed for 36 minutes with 6 individual exposures per field distributed over a circle of $10''$ of radius. The median seeing for all the fields is $0.64''$ (see figure 2) and the limiting magnitude is $I_{AB} \sim 24.5 - 25$.

Each image was overscan corrected, bias subtracted and flatfielded with a superflat computed with the exposures of the same night. No fringe correction was necessary. The FORS1 images get through a four port readout, so we treated separately the image subsets coming from the four quadrants of the CCD. Then we normalized the gain of the different subsets to obtain an image with an homogeneous background. Finally, we aligned the six individual exposures to produce the final coadded image. An example is given in figure 3.

At this stage, the images are ready for weak lensing analysis. The incoming light, crossing the atmosphere and getting through the optical system of the telescope, undergoes a smearing and a circularization. If we define the ellipticity of the source as

$$\mathbf{e} = \left(\frac{I_{11} - I_{22}}{Tr(I)}; \frac{2I_{12}}{Tr(I)} \right) \quad \text{with} \quad I_{ij} = \int d^2\theta W(\theta) \theta_i \theta_j f(\theta), \quad (1)$$

the observed ellipticity can be expressed by the KSB formalism^{6, 7, 8},

$$\mathbf{e}^{obs} = \mathbf{e}^{source} + P_\gamma \gamma + P^{sm} \mathbf{p} \quad (2)$$

where \mathbf{e}^{source} is the intrinsic ellipticity of the source, P^{sm} is the smear polarizability tensor associated with the effects produced by the anisotropic part of the point spread function (PSF from now on) and \mathbf{p} is connected to the anisotropic kernel $g(\theta)$ of the PSF through the two equations:

$$\mathbf{p} = (q_{11} - q_{22}; 2q_{12}); \quad q_{lm} = \int d^2\theta \theta_l \theta_m g(\theta). \quad (3)$$

The vector \mathbf{p} can be computed from the stellar ellipticity \mathbf{e}^*

$$p_\alpha = \frac{e_\alpha^*}{P_{\alpha\alpha}^{sm}}. \quad (4)$$

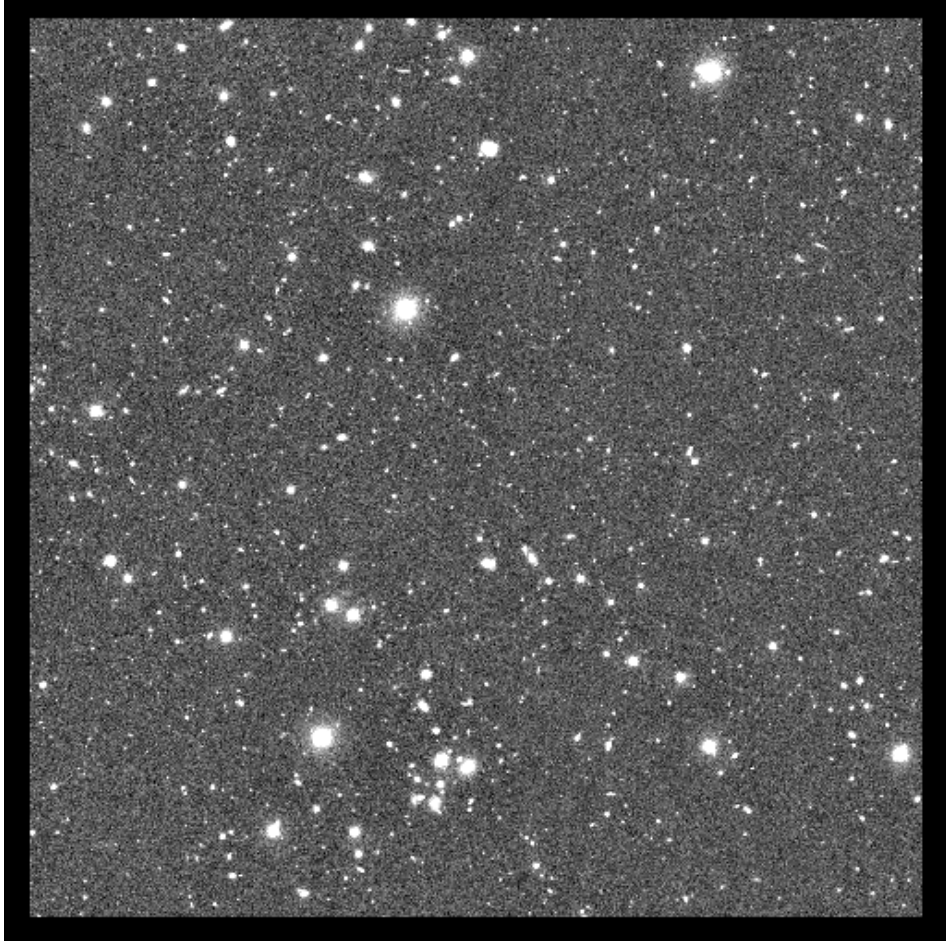


Figure 3: Final coadded image of a VLT field. In this case the seeing is $0.53''$, the source density is 35.3 sources/arcmin 2 , with a $6.5' \times 6.5'$ field and with 67 not saturated stars.

The quantity P_γ is the preseeing shear polarizability tensor, that takes into account both the effect of the gravitational shear and the circularization effect of the isotropic part of the PSF. It is given by the equation

$$P_\gamma = P^{sh} - \frac{P_\star^{sh}}{P_\star^{sm}} P^{sm} \quad (5)$$

where P^{sh} is the shear polarizability tensor and the subscript “ \star ” refers to the quantity computed for stars.

Assuming that there is no preferred direction for the intrinsic ellipticity of the sources, the cosmic shear at a given angular scale is

$$\gamma = \langle P_\gamma \rangle^{-1} \cdot \langle \mathbf{e}^{obs} - P^{sm} \mathbf{p} \rangle \quad (6)$$

where the average is computed over a given angular scale.

Two main tasks can be identified in shear computation:

- separation between stars and galaxies and selection of stars to compute the PSF correction for the galaxies;

- selection of galaxies for which the ellipticity can be computed with a small error.

Practically, this is translated in the following steps (for details, see²).

a) *Masking of images*: we remove all the boundaries of the four quadrants of the CCD. this

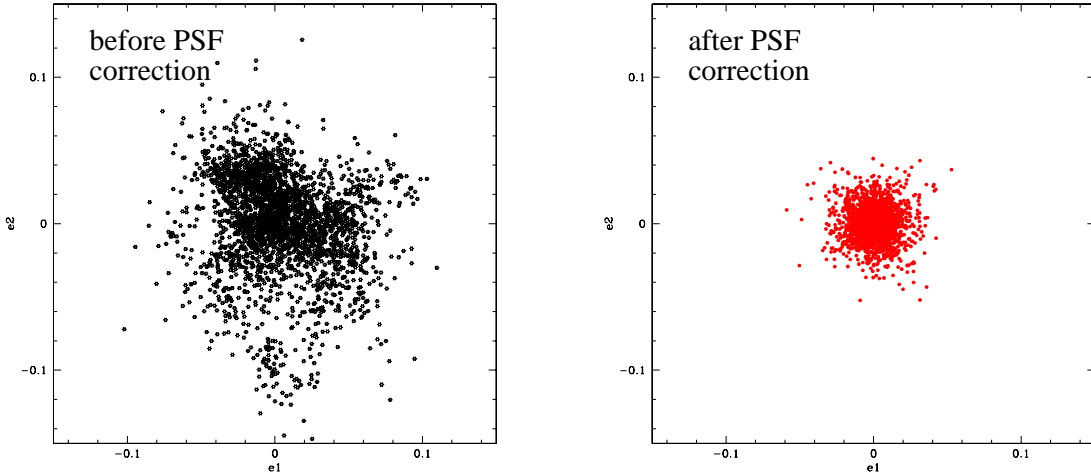


Figure 4: Star ellipticities before (at right) and after (at left) the PSF correction, for all the 45 selected VLT fields. A good PSF correction implies a zero mean value for e_1 and e_2 with small symmetric fluctuations.

includes the external boundaries and the central cross delineating the four quadrants. We remove also all sources too close to bright sources that can deform them, satellite traces and in general all those sources whose shape is difficult to compute correctly. About 12% of objects are removed in this way.

b) *Stars selection*: as usual, we use a radius vs magnitude plot to select not saturated stars. A low cut in the magnitude or an high cut in the radius would result in selecting small galaxies instead of stars therefore producing lower quality PSF corrections.

c) *Fit of the stellar polarizability tensors*: using stars, we compute $p_\alpha = \frac{e_\alpha^*}{P_{\alpha\alpha}^{sm}}$ and $\frac{P_{*}^{sh}}{P_{*}^{sm}}$ in all the image, fitting with a third order polynomial.

d) *P^γ computation*: using the stellar fits, we compute Eq. 5 for all the sources. P^γ is a very noisy matrix with huge fluctuations. For a given source, we then compute P^γ making an average among its values for the 30 nearest neighbors (see van Waerbeke *et al.*, 2000).

e) *Source selection*: we select sources with stellar class (given by SExtractor) < 0.9 , with radius $>$ stellar radius and with separation > 10 pixels.

In figure 4 we plot the star ellipticities for all VLT fields before and after the PSF correction. Five fields had a poor PSF correction and were eliminated.

At the end we have 45 fields with in average 60 stars/field (a minimum of 20 and a maximum of 120); we have roughly 58700 sources for 1900 arcmin² that is ~ 31 sources/arcmin² and 1300 sources/field.

3 Results and conclusion

For each final corrected image, we computed the variance of the shear, $\langle \gamma^2 \rangle$, at different angular scales, where the angular scale is given by the angular dimension of the top-hat window function. Then we made an average of $\langle \gamma^2 \rangle$ over the 45 fields.

In this way we can associate an error to the value of $\langle \gamma^2 \rangle$ at a given scale. It is important to stress that with 45 fields this also includes the cosmic variance.

In figure 5 we plot our results together with those of the other cosmic shear measurement projects. Note the remarkable agreement between the VLT and the CFHT results, although they were obtained with different observational strategies. This is the best guarantee that cosmic shear measurement is not associated with any local systematic effect.

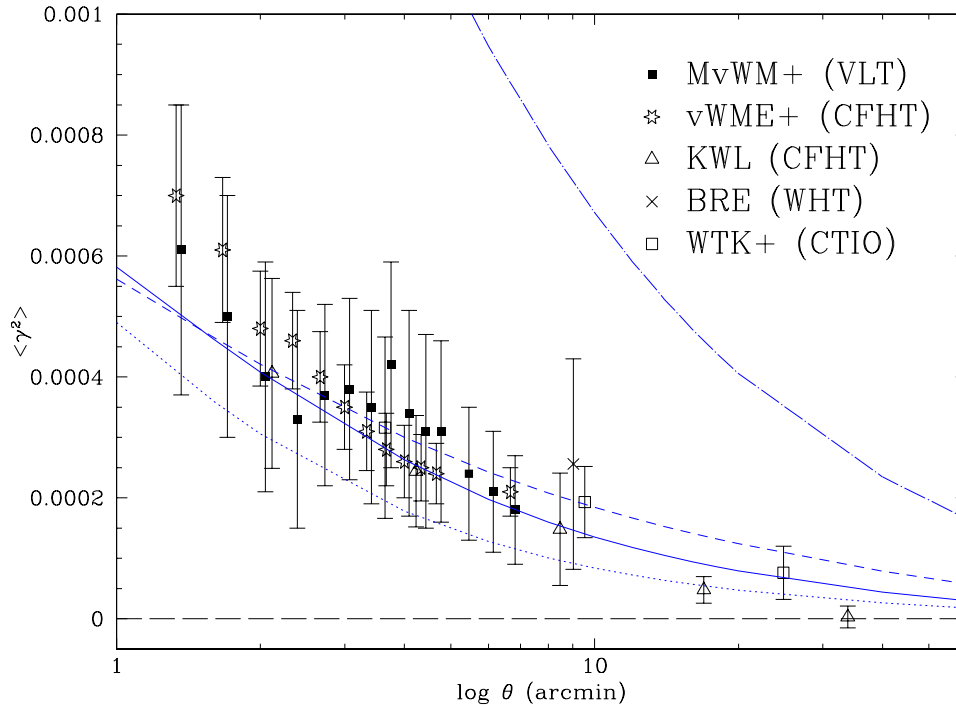


Figure 5: Summary of cosmic shear measurements. This work is referred as MvWM+. Some predictions of current models are also plotted, assuming sources $z_{eff} = 1$. The solid line corresponds to λ CDM, with $\Omega_m = 0.3$, $\lambda = 0.7$, $\Gamma = 0.21$; the dot-dashed line corresponds to COBE-normalized SCDM; the dashed line corresponds to cluster-normalized SCDM and the dotted line corresponds to cluster-normalized Open CDM with $\Omega_m = 0.3$.

Different theoretical models are also plotted in the figure. This plot rules out COBE-normalized standard CDM, which show the important potential of cosmic shear for cosmology. However, the errors are still too large to give precise predictions on the value of cosmological parameters Ω_0 and Λ and the shape of the power spectrum of primordial density fluctuations. Only a larger amount of data together with a complete control of the systematics will allow to reach this important goal.

Acknowledgments

We thank the ESO service observing team at the VLT for performing the observations. We thank V. Charmandaris (Dr IRAF), D. Bacon and A. Refregier for helpful discussions. This work was supported by the TMR Network ‘‘Gravitational Lensing: New Constraints on Cosmology and the Distribution of Dark Matter’’ of the EC under contract No. ERBFMRX-CT97-0172.

References

1. P. Schneider *et al*, *Astr. & Astrophys.* **333**, 767 (1998).
2. L. van Waerbeke *et al*, *Astr. & Astrophys.* **358**, 30 (2000).
3. D. Bacon, A. Refregier & R. Ellis, *MNRAS submitted*, astro-ph/0003008.
4. D. Wittman *et al*, *Nature* **405**, 143 (2000).
5. N. Kaiser, G. Wilson & G. Luppino, *Astrophys. J. submitted*, astro-ph/0003338.
6. N. Kaiser, G. Squires & T. Broadhurst, *Astrophys. J.* **449**, 460 (1995).
7. G. Luppino & N. Kaiser, *Astrophys. J.* **475**, 20L (1997).
8. H. Hoekstra *et al*, *Astrophys. J.* **504**, 636 (1998).